4
NMR investigation of cyclodextrin based supramolecular drug delivery system: Part II

4.1 INTRODUCTION

Extensive use of β-CD as encapsulating agent is due to its ease of availability and cheap production methods. However, low solubility and considerable renal toxicity limit its uses in pharmaceutical formulations [Gould and Scott, 2005]. Consecutively synthesis and marketization of various kinds of β-CD derivatives such as methylated β-CD, hydroxy alkylated β-CD and acetylated β-CD have been considered to enhance the solubility and inclusion efficiency of β-CD as drug carriers [Anjana et al., 2013]. Among these different derivatives 2-hydroxypropyl-β-cyclodextrin (HP-β-CD) exhibits high aqueous solubility and minimal renal toxicity compared to the β-CD molecule [Uekama, et al., 1998; Zhang and Ma, 2013]. As a matter of fact commercial market of pharmaceutical products containing HP-β-CD with various active ingredients has seen fair growth in USA and Europe [Brewster and Loftsson, 2007; Malanga et al., 2016].

Similar to the β-CD inclusion complexes, there are no reports available either describing molecular mobility of the encapsulated drug or extracting the internuclear distances between the drug and the carrier in case of HP-β-CD inclusion complexes. However, NMR has been widely used in the characterization of such inclusion complexes of HP-β-CD. Veiga et al. has reported the conformational study of the inclusion complex of tolbutamide with HP-β-CD using ^{1}H chemical shift, intermolecular NOE and computational molecular modelling [Veiga et al., 2001]. Sinha and co-workers have characterized the celecoxib (CXB):HP-β-CD complex by using ^{1}H-NMR and monitored the chemical shift changes induced in CXB due to complexation [Sinha et al., 2011]. Further, Garg and co-workers have reported implementation of 2D-ROESY experiment for the inclusion complex of eugenol in HP-β-CD to evaluate the complexation mode and spatial arrangement of guest inside the host [Garg et al., 2010]. Besides ^{1}H NMR studies, Mura et al. employed ^{13}C NMR experiments that suggested the evidence of partial inclusion of ascorbic acid inside the HP-β-CD [Mura, 2014]. The literature review therefore clearly indicated a requirement of understanding the dynamic behavior of an encapsulated drug molecule within HP-β-CD cavity by utilizing NMR methods as described in Chapter 3. Moreover, it also appeared to be interesting to compare the findings with the parent β-CD carrier.

Hence, in this chapter we report application of selective spin-lattice relaxation rate measurement based approaches to characterize HP-β-CD complexes along with a comparative analysis with respect to β-CD complexes followed by pointing out the relevant drawbacks in employing such methods in case of HP-β-CD. It is observed that the bi-selective relaxation rate measurement method is not appropriate in case of HP-β-CD. HP-β-CD being a mixture of isomers with various degrees and pattern of hydroxyl-propylation, gives rise to unresolved H_3 proton peak [José et al., 2001] causing accurate measurement of R_1^{bs} difficult since achievement of bi-selective excitation is not possible in such overlapped peak situation. We have chosen diflunisal (DFL) as the model drug molecule to study encapsulation in HP-β-CD and β-CD in

view of extracting the interproton distances. The binding parameters for DFL_CD complexes have already been investigated in order to enhance its oral bioavailability using titration equilibrium dialysis, microcalorimetric and potentiometric methods that have suggested 1:1 stoichiometry of DFL_CD complexes [Magnusdottir et al., 2002; Loftsson et al., 2004; Másson et al., 2003; Ugwu et al., 1999]. Since the binding parameters and stoichiometry of these complexes are already available in literature, we did not perform the NMR titration experiments for these complexes. In the present study we have prescribed the most favorable set of 1D selective experiments based on NMR relaxation and NOE to quantify internuclear distances in view of the molecular system and respective spectral complexity in case of β-CD and HP-β-CD inclusion complexes. The study mainly focusses to understand the mode of insertion of DFL inside the cyclodextrin cavity by looking at the internuclear distances within the encapsulated environment. Although, 1D quantitative NOE experiments as well as selective relaxation measurements are well-established methods from last several years, the full potential of these methods is hardly used for the structural studies of supramolecular inclusion complexes. The experimental findings have been further confirmed by DFT calculations.

f

4.2 METHODOLOGY

Changes in chemical shift and proton spin-lattice relaxation rates have been monitored to characterize the inclusion complexes of DFL with β-CD and HP-β-CD as stated in Chapter 3. Two different sets of experiments were performed, one based on selective spin-lattice relaxation rate and the other based on NOE enabling extraction of interproton distance and correlation time for the complexes. A series of 1D selective Rotational Overhauser Enhancement SpectroscopY (ROESY) has been performed to quantify the interproton distances in case of HP-β-CD encapsulated DFL. Furthermore, to detect the dipolarly coupled proton network in CD encapsulated DFL, 2D ROESY experiments were recorded.

4.2.1 1D selective ROE measurements

Due to unresolved H_3 proton peak [José et al., 2001] of HP-β-CD, we adopted the 1D selective ROE experiments for the interproton distance measurement [Butts et al., 2011; Chini et al., 2012; Halbeek and Poppe, 1992; Poveda et al., 1997] in case of DFL_HP-β-CD complex. A stable encapsulated molecular system with restricted molecular mobility of DFL within the cavity is assumed, allowing to treat the complex as a single molecular entity. Hence, interproton distances of DFL protons and H_3 proton of HP-β-CD were extracted using the known internal distance of DFL H_5-H_6 as a reference by employing a set of 1D selective ROESY experiments. 1D selective ROESY experiments exploit selective refocussing of DFL protons followed by a spinlock segment that allows transfer of magnetization from selectively refocused DFL protons to that of HP-β-CD cavity protons.

The internucler distances (r_{ij}) were then extracted using the intensity ratio method [Ammalahti et al., 1996] with inclusion of spin lock pulse offset correction factors (c_{ij}) as explaineded by Ammalahti et al. It has been shown in their paper for 2D ROESY experiment that the internuclear distances may be determined from the diagonal and cross peaks intensities, a_{ij} and a_{ii}, respectively, using Eq. 4.1.

$$r_{ij} = r_{ref}\left(\frac{a_{ref}c_{ref}}{a_{ij}c_{ij}}\right)^{\frac{1}{6}} \quad \text{.....(4.1)}$$

Where

$$c_{ij} = \frac{1}{\sin^2\theta_i \sin^2\theta_j}; \tan\theta_i = \frac{\gamma B_1}{(\omega_i - \omega_o)}$$

Where $(\omega_i - \omega_0)$ is the chemical shift difference between the peak and offset o_1p (in Hz) and γB_1 is the spin lock power. A detailed explanation of these equations and their utility in calculating internuclear distances is reported in the literature by Ammalahti and co-workers. The internuclear distances between DFL protons with H_3 proton of HP–β–CD determined by 1D ROESY experiments were comparable with computationally derived distances.

4.2.2 DFT calculations

Density functional theory (DFT) quantum chemistry calculations were performed to support the experimental data, in particular, minimum energy geometries and energies. Then the guest molecule was placed inside the CD cavity at different positions and geometry optimization was repeated. Four different initial configurations were formed *viz.*, [a] DFL fluorine group (–F) outside the β-CD cavity (orientation AA) [b] DFL fluorine group (–F) inside the β-CD cavity (orientation AB) [c] DFL fluorine group (–F) outside the HP-β-CD cavity (orientation AA') [d] DFL fluorine group (–F) inside the HP-β-CD cavity (orientation AB'). These orientations can be visualized similar to the cartoon representation given in Figure 3.4.

4.3 EXPERIMENTAL SECTION

4.3.1 Materials

Diflunisal (2',4'-difluoro-4-hydroxybiphenyl-3-carboxylic acid), HP-β-CD and D_2O (99.9%) were purchased from Sigma-Aldrich while β-CD was obtained from Alfa Aesar. All chemicals were used without further purification. Figure 4.1 represents the molecular structure of diflunisal (DFL) with numbering of protons (denoted as 2-5) and that of β-CD/ HP-β-CD. 2 mM solutions of 1:1 host-guest complex of DFL with both the β-CDs were made in 0.5 mL D_2O for NMR measurements. Nitrogen purging was carried out to remove dissolved oxygen from all the samples before relaxation and NOE measurements.

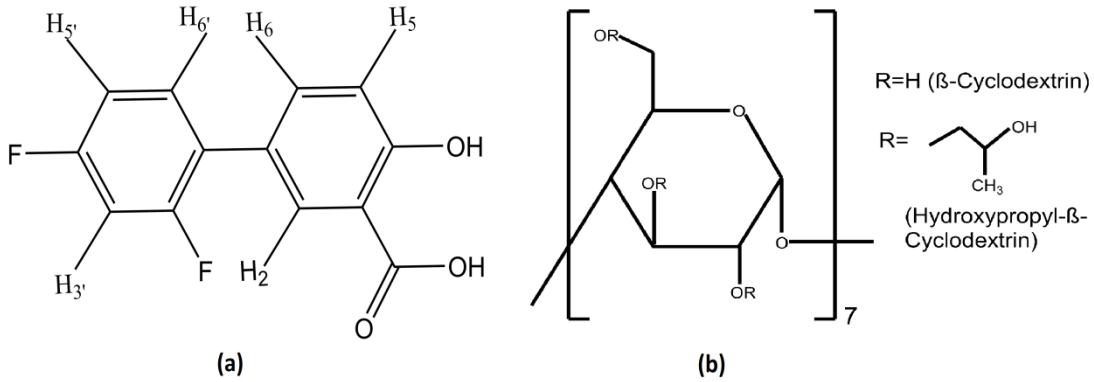

Figure 4.1 : Chemical Structure of (a) Diflunisal (b) β-CD and HP-β-CD

4.3.2 Technical details of NMR experiments

All the NMR spectra were recorded on a Bruker Ascend 500 MHz WB NMR spectrometer equipped with a BBFO probehead. The probe temperature was maintained at 300 K for all the experiments. Chemical shifts were referenced to the residual solvent signal of HDO at 4.69 ppm. 1D selective ROESY spectra were recorded using the Bruker SELROGP pulse sequence (Chapter 2, Figure 2.8). 2D ROESY experiments were recorded with standard Bruker pulse program ROESYPH (Chapter 2, Figure 2.7). All the experimental parameters used for the NMR relaxation and 1D ROESY experiments are given in Table 4.1.

Table 4.1: Experimental parameters used for the relaxation and 1D ROESY experiments.

Acquisition Parameter	Relaxation	1D ROESY
^{1}H hard π/2 pulse parameters	14.15 µs, – 11.76 dB	14.15 µs, – 11.76 dB
Shaped pulse (Gaussian) parameters	10 ms; 31.48 dB	40 ms; 35.54 dB
Spectral width (SW)	10.0 ppm	10.0 ppm
Data points (Td)	32 k	32 k
Repetition time (d1)	15 s	15 s
No. of scans (NS)	8	3200
Recovery periods (τ) / ROESY spin lock period (τ_m)	0-20 s	400 ms

4.3.3 Computational details

Exactly same approach was followed for the DFT calculations required for the DFL_β-CD and DFL_HP-β-CD systems as described in section 3.3.3. Initial guess geometries for β-CD and HP-β-CD molecules were taken from RCSB protein data bank (PDB) for geometry optimizations. The calculations were performed using the GAMESS electronic structure theory program [Schmidt et al., 1993]. Results of the DFT calculations are compared with experimental measurements in section 4.4.4.

4.4 RESULTS AND DISCUSSION

4.4.1 Chemical shifts, peak intensities and presence of NOE cross peaks

Figure 4.2 represents the stack plot of the ^{1}H NMR spectra of free DFL (a), DFL_β-CD (b) and DFL_HP-β-CD (c) complexes (1:1) in D_2O recorded at 300 K. Significant upfield and downfield shift of the different ^{1}H NMR chemical shifts, and enhanced peak intensities for all DFL protons were observed for the CD complexes compared to free DFL in solution. The chemical shift values of all the DFL protons in free and encapsulated state have been documented in Table 4.2. The shift in chemical shift values clearly indicated change in electronic environment of DFL upon encapsulation. Further, the increase in peak intensity could also be associated with the enhanced solubility achieved due to encapsulation. The peak intensities observed for the DFL_HP-β-CD complex were further enhanced compared to that of DFL_β-CD complex, suggesting higher solubility of DFL in hydrophilic HP-β-CD. It was also noted that after encapsulation the merged protons of free DFL namely H_3/H_5 on the fluorinated ring and H_5 on the non-fluorinated ring become considerably resolved. This effect is significantly higher in case

of HP-β-CD. This observation could be explained by stating that the above mentioned protons are located in two different rings of DFL. Presumably encapsulation of DFL proceeds via the non-fluorinated ring where H_5 resides and therefore it experiences a higher change in chemical environment resulting greater separation of chemical shift value from the other two protons residing on the fluorinated ring.

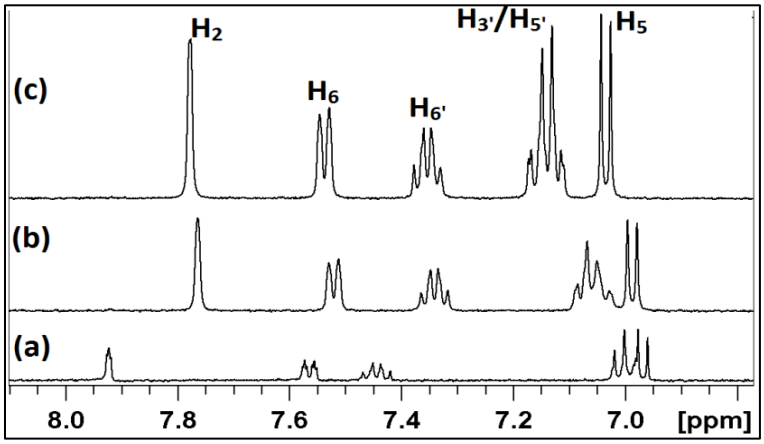

Figure 4.2 : Plot of ^{1}H NMR spectra of Diflunisal protons in (a) Free DFL (b) DFL_β-CD complex (c) DFL_HP-β-CD complex recorded at 300 K.

Table 4.2 : Chemical shifts of the DFL protons in free and encapsulated state.

Proton	Free DFL (δ_{ppm})	DFL_β-CD (δ_{ppm})	DFL_HP-β-CD (δ_{ppm})
H_2	7.923	7.767	7.778
H_6	7.564	7.517	7.538
$H_{6'}$	7.444	7.343	7.354
$H_{3'/5'}$	6.989 (Merged)	7.058	7.139
H_5	6.989	6.982	7.035

Existence of intermolecular NOEs (cross peaks) between the H_3 protons of CDs and the ring protons of DFL in the traditional 2D ROESY spectra of 1:1 DFL_β-CD and DFL_HP-β-CD complexes as shown in Figure 4.3 compliments the chemical shift data confirming encapsulation.

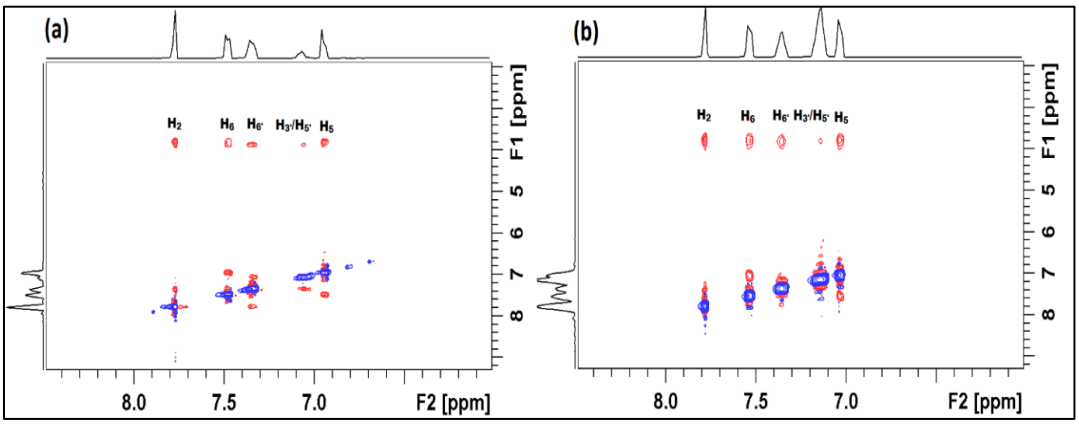

Figure 4.3 : 2D ROESY spectra of (a) DFL_β-CD complex and (b) DFL_HP-β-CD complex recorded with τ_m=400 ms at 300 K.

4.4.2 Molecular Rotational correlation times (τ_c)

In this section, we report the measurement of R_1^{ns} and R_1^{se} rates for DFL_CD complexes and compared the same with that of free DFL to confirm encapsulation. Similar to the molecules paracetamol and aspirin reported in Chapter 3, for free DFL τ_c was calculated directly from the selective relaxation rate (R_1^{se}), whereas for the drug bound to β-CD or HP-β-CD the plot of the ratio R_1^{ns}/R_1^{se} *vs* $\omega\tau_c$ was used to quantify τ_c by extrapolation method. Non-selective and selective relaxation rates and corresponding τ_c have been tabulated for each proton of DFL in free and encapsulated state in Table 4.3 and Table 4.4.

The ratio of R_1^{ns}/R_1^{se} equals to 1.05 for an intermediate motional regime ($\omega\tau_c$ ~1) for a pure dipole-dipole relaxation mechanism as discussed in Chapter 3. In the present case for DFL encapsulated in β-CD or HP β-CD, the ratio of R_1^{ns}/R_1^{se} is close to the theoretically expected value which suggested that after the encapsulation in CD cavity the drug has entered the intermediate motion regime. The experimentally derived correlation times for the free drug (average $\tau_c = 1.26\times10^{-10}$ s) increased significantly in the presence of β-CD (average $\tau_c=2.46\times10^{-9}$ s) or HP-β-CD (average $\tau_c=2.83\times10^{-9}$ s) confirming the formation of inclusion complexes between them.

Table 4.3 : Chemical shift and molecular rotational correlation time measured for selected protons of DFL in free state at T=300 K.

Free DFL			
Protons	**δ_{ppm}**	**R_1^{se} (s^{-1})**	**τ_c (s)**
H_2 (s)	7.923	0.237±0.007	$(8.70\pm0.11)\times10^{-11}$
H_6 (d)	7.564	0.382±0.024	$(1.39\pm0.09)\times10^{-10}$
$H_{6'}$ (q)	7.444	0.413±0.028	$(1.52\pm0.16)\times10^{-10}$

Table 4.4 : Chemical shift and molecular rotational correlation time measured for selected protons of DFL_β-CD and DFL_HP-β-CD complex at T=300 K.

DFL_β-CD complex					
Protons	**δ_{ppm}**	**R_1^{ns} (s^{-1})**	**R_1^{se} (s^{-1})**	**R_1^{ns}/R_1^{se}**	**τ_c (s)**
H_2 (s)	7.767	0.526 ±0.031	0.530 ±0.034	0.992 ±0.020	$(2.28\pm0.06)\times10^{-9}$
H_6 (d)	7.517	0.549 ±0.035	0.619 ±0.044	0.887 ±0.015	$(2.77\pm0.04)\times10^{-9}$
$H_{6'}$ (q)	7.343	0.570 ±0.041	0.620 ±0.043	0.919 ±0.011	$(2.60\pm0.09)\times10^{-9}$
H_5 (d)	6.982	0.555 ±0.033	0.551 ±0.041	1.007 ±0.029	$(2.20\pm0.03)\times10^{-9}$
DFL_HP-β-CD complex					
H_2 (s)	7.778	0.519 ±0.027	0.551 ±0.036	0.942 ±0.023	$(2.51\pm0.09)\times10^{-9}$
H_6 (d)	7.538	0.556 ±0.037	0.662 ±0.061	0.839 ±0.019	$(3.07\pm0.11)\times10^{-9}$
$H_{6'}$ (q)	7.354	0.594 ±0.045	0.731 ±0.089	0.812 ±0.009	$(3.14\pm0.08)\times10^{-9}$
H_5 (d)	7.035	0.546 ±0.033	0.597 ±0.049	0.914 ±0.031	$(2.62\pm0.18)\times10^{-9}$

4.4.3 Interproton distance measurement

It is beneficial to attempt determination of interproton distances for a molecule encapsulated within cyclodextrin cavity for understanding the mode of insertion of the molecule inside such cavity. Host-guest complexation or insertion of a molecule within the CD cavity depends on a variety of interaction ranging from electrostatic, hydrophobic, van der Waals and hydrogen bonding. These interactions determine the complex life time during which the

host-guest can be considered to be a single molecular entity. With such an assumption, interproton distance measurements can be attempted employing NMR methods as demonstrated in Chapter 3. The interproton distances can then directly indicate the mode of insertion of the guest in terms of functional groups or part of the guest entering the cavity. In this section our main focus is to determine interproton distances for the two different DFL_CD complexes and deliver a comparative analysis of the NMR methods utilized.

It is well known in literature that insertion of a molecule within CD cavity mainly alters the chemical shifts of inner protons of CD (H_3 and H_5) [Salvatierra et al., 1996] Therefore, interproton distance between the guest molecule and the CD inner protons indicate the part of the molecule through which it enters the cavity. However, such distance measurement is meaningful only when a simple isotropic motional model described with a single correlation time is considered for the complex as a whole. This directs that mobility of the molecule within the cavity is considered to be restricted. In contrast to the previous two molecular systems described in Chapter 3 namely Paracetamol_β-CD and Aspirin_β-CD, the inter proton distance measurement is attempted in case of DFL_CD complexes by exploiting two different 1D selective NMR approaches, one based on relaxation rate measurements as illustrated previously and second based on NOE method considering the spectral complexity of the encapsulated species.

In case of DFL_β-CD, with completely resolved proton peaks for both DFL and β-CD as shown in Figure 4.4a, the interproton distances were extracted using the cross relaxation rates (σ_{ij}) determined from the experimentally measured bi-selective and selective relaxation rates as presented in Chapter 3 [Kumar et al., 2017]. A similar approach was not applicable in case of DFL_HP-β-CD due to unresolved proton peaks of HP-β-CD as shown in Figure 4.4b hindering simultaneous inversion of the HP-β-CD and DFL protons by a bi-selective pulse. Under these circumstances, the ^1H-^1H distances were determined using 1D selective ROESY method. In the following two sections, a brief account of the two methods have been provided in terms of the ease of quantification, requirement of a priory information related to molecular parameters and reliability.

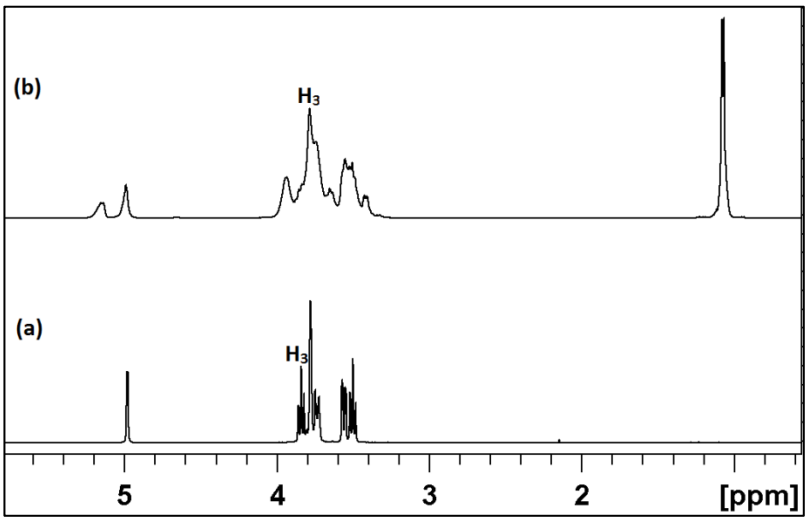

Figure 4. 4 : Plot of ^1H NMR spectra of cyclodextrins protons in (a) DFL_β-CD and (b) DFL_HP-β-CD complex recorded at 300 K.

(a) Cross relaxation rate (σ_{ij}) measurement in case of DFL_β-CD

In this case the interproton distances between DFL proton and the β-CD protons were evaluated from molecular rotational correlation time (τ_c) and cross relaxation rate (σ_{ij}). Both τ_c and σ_{ij} were experimentally extracted from ^1H non-selective, selective and bi-selective relaxation rate measurements. The cross-relaxation rate (σ_{ij}) of a chosen DFL proton was extracted from bi-selective and selective relaxation rate as discussed in Chapter 3 where R_1^{se} was measured by employing selective inversion of the DFL proton while R_1^{bs} was extracted from bi-selective inversion recovery experiment in which the chosen DFL proton has been simultaneously inverted with the H_3 proton of β-CD. Figure 4.5 is a representative linear fitting plot of bi-selective relaxation rate (R_1^{bs}) measurement for H_5 proton of DFL using Eq. 3.7 considering the initial rate approximation. Finally Eq. 2.28 (chapter 2) has been used to evaluate the desired interproton distance by inserting the experimentally determined τ_c and σ_{ij}. Table 4.5 consolidates the experimentally measured bi-selective relaxation rates, the corresponding cross-relaxation rates extracted for the DFL protons, the experimentally derived interproton distances and the theoretically calculated interproton distances for the DFL_β-CD complex.

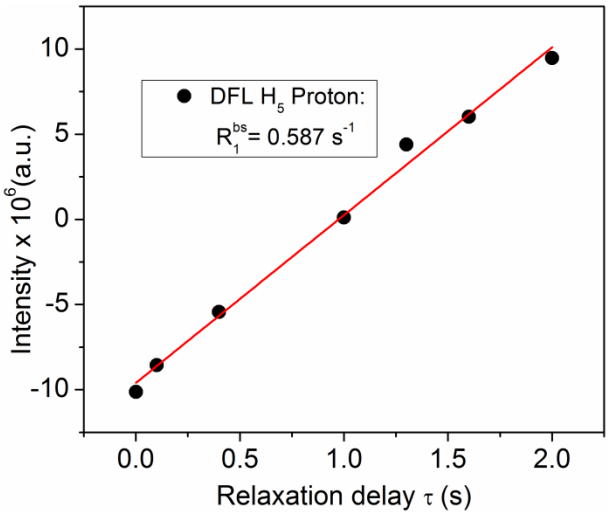

Figure 4.5 : Linear fitting plot of DFL H_5 proton to extract R_1^{bs} considering the initial rate approximation.

(b) 1D selective ROE measurements in case of DFL_HP-β-CD

We adopted 1D Selective ROESY experiment for extracting the interproton distances in case of DFL_HP-β-CD complex. In 1D selective ROESY experiment, selective refocusing of one of the DFL proton followed by spin locking in the transverse plane transfer the magnetization from the said DFL proton to the dipolarly connected protons in the complex giving rise to significantly measurable cross peak intensities with H_3 proton of HP-β-CD as well as with the adjacent DFL proton. To evaluate the desired interproton distances of the DFL_HP- β-CD complex, DFL H_5-H_6 interproton spatial distance was used as the reference and was obtained from the optimized MOLDEN structure of DFL. Figure 4.6 is the representative 1D ROESY spectrum of DFL_HP-β-CD complex with selective refocusing of DFL H_5 proton. It is clearly seen from Figure 4.6 that selective refocusing of DFL H_5 proton generates cross peak with H_3 proton of HP-β-CD and H_6 proton of DFL. Experimentally measured cross peak intensities along with the theoretically derived DFL H_5-H_6 reference distance is plugged in to Eq. 4.1 to extract the interproton distance between H_5 proton of DFL and H_3 proton of HP-β-CD. Similar experimental data were acquired for all the DFL protons and calculations of interproton distances were carried out. The interproton distances obtained from both 1D selective ROESY experiment and quantum mechanical calculations for DFL_HP-β-CD complex are documented in Table 4.5.

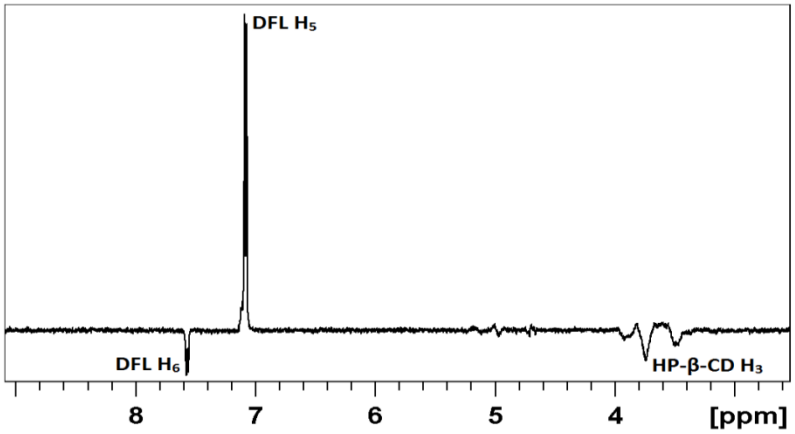

Figure 4.6 : 1D ROESY spectrum of DFL_HP-β-CDcomplex with selective refocusing of DFL H_5 proton.

Critical inspection of Table 4.5 revealed a number of interesting facts. The bi-selective relaxation rates measured in case of DFL_β-CD complex is of the same order of that of the selective relaxation rate resulting in very small cross relaxation rates observed for each proton. Such small cross relaxation rates can be attributed to the fact that the complexes are of intermediate size and therefore σ_{ij} falls in the cross over region at the working magnetic field of 11.7 T. This was expected following our observations made in case of paracetamol and aspirin β-CD complexes in Chapter 3. The sign of the cross-relaxation rates are negative in case of DFL_β-CD complex indicating dominant contribution of W_0 (zero quantum) relaxation mechanism as discussed in literature [Kumar et al., 2017]. This set of distances calculated from such very small σ_{ij} values measured at high magnetic field with large experimental errors has limited credibility. However, the trend observed for these distances is worthy enough to predict the mode of insertion of DFL in to the CD cavity.

In the present case the interproton distances measured between H_3 proton of β-CD with DFL H_2, H_5, H_6, and $H_{6'}$ protons are 3.84, 2.96, 2.83 and 4.32 Å respectively. The same could not be reported for DFL $H_{3'}$ and $H_{5'}$ protons due to peak overlap hindering the required selective inversion of these protons. It is to be pointed out that relatively shorter distances were measured between β-CD H_3 proton with DFL non-fluorinated ring protons (H_2, H_5 and H_6) compared to the fluorinated ring proton ($H_{6'}$).

Table 4.5 : Interproton distance measured for selected protons of DFL_β-CD and DFL_HP-β-CD complexes.

DFL_β-CD complex				
Proton	H_2 (s)	H_6 (d)	$H_{6'}$ (q)	H_5 (d)
R_1^{bs} (s^{-1})	0.522 ± 0.029	0.559 ± 0.037	0.615 ± 0.044	0.587 ± 0.038
σ_{ij}	-0.008± 0.031	-0.060± 0.040	-0.005± 0.043	-0.036±0.039
r_{ij} (Å)	3.836 ± 0.27 (3.496)*	2.832±0.07 (2.516)*	4.317±0.15 (4.963)*	2.961±0.29 (3.205)*
Abs % error†	9.72	12.55	13.01	7.61
DFL_HP-β-CD complex				
r_{ij} (Å)	2.226±0.09 (2.630)*	2.822±0.11 (3.160)*	4.660±0.18 (4.801)*	2.551±0.015 (2.599)*
Abs % error†	15.36	10.70	2.93	1.84

***** Intermolecular proton distances computed by density functional theory.

† $|\%error| = \left| r_{theoretical} - r_{experimental} \right| / r_{theoretical}$

The interproton distances calculated in case of DFL_HP-β-CD from the set of 1D selective ROESY experiments are devoid of the problems faced in case of relaxation measurement at high magnetic field. However, in case of selective ROESY, a series of experiments for a single proton at different mixing times was required to confirm the initial linear behavior of the cross peak intensity build up. This certainly increased the amount of time consumed to set up the 1D selective ROESY experiments. Except DFL H_2 proton, the other DFL proton distances were similar to that of DFL_β-CD complex. A comparatively shorter distance measured in case of DFL H_2 proton could be due to a different geometry adopted by DFL while entering the HP-β-CD cavity.

Further, a careful comparison of distance data generated in each case using two different methods was also drawn in terms of the % deviation from the theoretically predicted distances (discussed in the following section) for the most stable conformations of the two complexes. It was found that on an average the interproton distances measured in case of DFL_HP-β-CD using 1D selective ROESY have better concurrence with the theoretical values than in case of DFL_β-CD interproton distances measured using selective relaxation rates.

4.4.4 Proposed structure of the inclusion complexes

A detailed analysis of experimentally derived interproton distances supported by theoretically predicted distances enabled us to propose the mode of insertion of DFL inside both the CD cavities and a possible geometry of the inclusion complexes. Shorter interproton distances measured for the non-fluorinated ring proton of DFL with the CD proton indicated entry of the molecule through the non-fluorinated ring while the fluorinated ring remained outside the cavity. The observed downfield shift (as indicated by a preliminary inspection of the spectrum through naked eye) in the chemical shift of DFL H_5 proton probably suggests possibility of hydrogen bonding interaction between –OH group of DFL and H_6 proton of β-CD (lower rim) causing deshielding effect due to lowering of electron density near the DFL H_5 proton. This observation further strengthens the proposed inclusion geometry. A similar situation is also observed in case of DFL_HP-β-CD complex. Figure 4.7 denotes a cartoon representation of the host-guest structure. The experimentally proposed geometry of inclusion is further reinforced by DFT calculations.

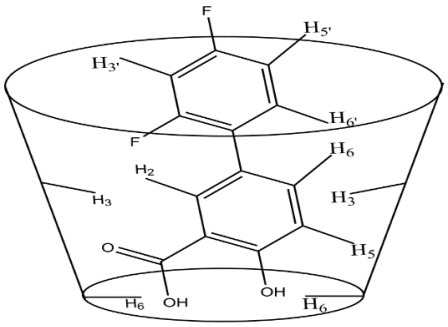

Figure 4.7 : Proposed geometry of DFL_CD complex based on experimental data.

Optimized geometries for the four different configurations mentioned earlier are shown in Figure 4.8. For the DFL_β-CD complex, the AA configuration is lower in energy (by 14.08 kcal/mol) as compared to the AB configuration and for the DFL_HP-β-CD complex, the AA' configuration is lower in energy (by 16.87 kcal/mol) as compared to the AB' configuration. These computed energy values are consistent with the experimental observations.

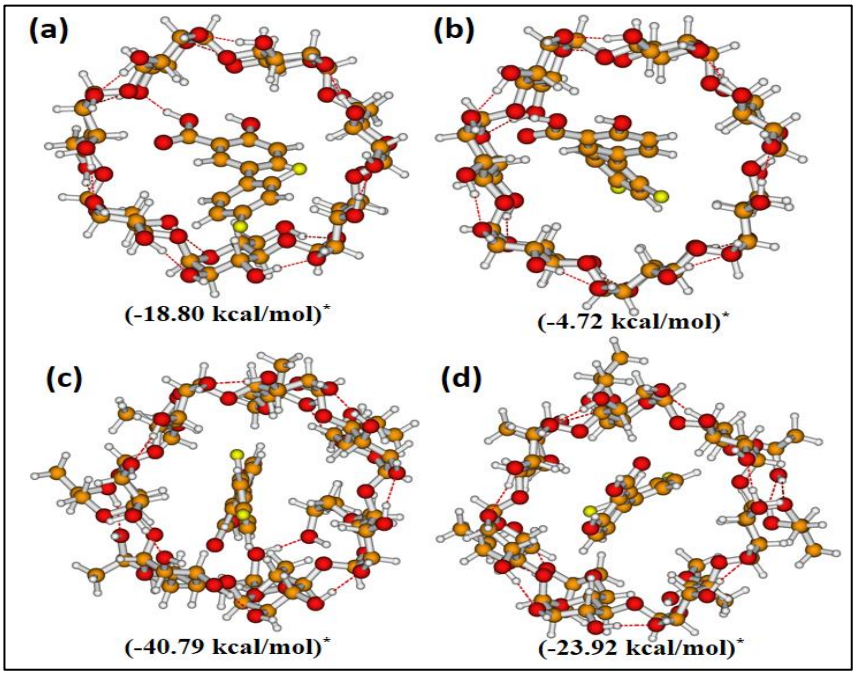

* Energies are relative to $E_{\beta\text{-CD/HP-}\beta\text{-CD}} + E_{drug}$ with β-CD/ HP-β-CD and the drug molecule infinitely separated.

Figure 4.8 : Optimized geometries for (a) Diflunisal –F group outside the β-CD cavity- AA (b) Diflunisal –F group inside the β-CD cavity- AB (c) Diflunisal –F group outside the HP-β-CD cavity- AA' (d) Diflunisal –F group inside the HP-β-CD cavity- AB'. The colors of the atoms are denoted as: C-Brown, O-Red, F-Lime and H-White.

Further, the interproton distances measured for DFL_β-CD and DFL_HP-β-CD complexes have the mean absolute % error of 10.71% and 7.70% respectively with respect to the distances determined from DFT calculations. As discussed in section 4.2.1, for interproton distance measurements we have assumed a stable encapsulated molecular system with minimal molecular mobility of DFL within the cavity. The lower mean absolute % error in case of DFL_HP-β-CD complexes thus support a more stable complexation between DFL and HP-β-CD resulting in the better match of experimental data with the theoretical one.

4.5 CONCLUSION

In this Chapter we have illustrated the applicability of two different 1D selective NMR methods based on selective relaxation and magnetization transfer to analyze cyclodextrin inclusion complexes. β-CD and HP-β-CD complexes of DFL, a fluorinated drug were used to demonstrate the pros and cons of these methods. Based on spectral complexity of the complexes the appropriate method is prescribed for interproton distance measurement and prediction of mode of insertion of the drug. It was found that both kinds of experiments are applicable to study host-guest inclusion complexes. However, both the methods offer subtle advantages and also pose experimental shortcomings. A comparative of the two methods at the backdrop of β-CD inclusion complexes can be drawn as follows:

- A set of selective relaxation rate measurements are more informative by quantifying both interproton distances and correlation time of the molecular system. The major advantage of this method is that no prior knowledge of any other interproton distance is required. However, this method is applicable only in case of spectra with well resolved peaks.
- On the other hand, 1D Selective NOE based measurements are easy to set up and convenient to extract the interproton distances for the molecular systems with unresolved peaks. One may choose to use superior ROESY methods such as EASY

ROSEY [Thiele et al., 2009] or Offset-compensated and zero-quantum suppressed ROESY [Boros and Batta, 2016] for better distance determination. Nevertheless, a prior knowledge of reference interproton distance is an obligation.

- On a certain NMR instrument the relaxation based method is time efficient as these experiments require less number of scans *ca*. 8 while to observe a significantly intense ROE peak it requires *ca.* 3200 scans in case of low drug concentration. Further, to maintain the linear approximation of cross peak intensity build up, the optimization of appropriate mixing time requires considerable amount of machine time in the ROESY method. As a whole relaxation based analysis is far more time efficient.

In the present case it has been concluded that HP-β-CD is a superior encapsulating agent compared to β-CD for DFL. Higher cross peak intensities and shorter interproton distances for the non-fluorinated ring of DFL indicate the most probable mode of insertion of the molecule. In general it is possible to state that fluorinated moiety in a molecule would prefer to remain outside during complexation with CD cavities.

…